DNA Repair 22 (2014) 12–23

Contents lists available at ScienceDirect

DNA Repair

journal homepage: www.elsevier.com/locate/dnarepair

Sgs1 and Exo1 suppress targeted chromosome duplication during ends-in and ends-out gene targeting

Anamarija Štafa[a,b,*], Marina Miklenić[a], Bojan Žunar[a], Berislav Lisnić[a,1], Lorraine S. Symington[b], Ivan-Krešimir Svetec[a,*]

[a] Laboratory for Biology and Microbial Genetics, Department of Biochemical Engineering, Faculty of Food Technology and Biotechnology, University of Zagreb, Zagreb 10000, Croatia
[b] Department of Microbiology and Immunology, Columbia University Medical Center, New York, NY 10032, USA

ARTICLE INFO

Article history:
Received 19 February 2014
Received in revised form 5 July 2014
Accepted 9 July 2014

Keywords:
Gene targeting
Ends-in
Ends-out
Homologous recombination
Break-induced replication
Whole chromosome duplication

ABSTRACT

Gene targeting is extremely efficient in the yeast *Saccharomyces cerevisiae*. It is performed by transformation with a linear, non-replicative DNA fragment carrying a selectable marker and containing ends homologous to the particular locus in a genome. However, even in *S. cerevisiae*, transformation can result in unwanted (aberrant) integration events, the frequency and spectra of which are quite different for ends-out and ends-in transformation assays. It has been observed that gene replacement (ends-out gene targeting) can result in illegitimate integration, integration of the transforming DNA fragment next to the target sequence and duplication of a targeted chromosome. By contrast, plasmid integration (ends-in gene targeting) is often associated with multiple targeted integration events but illegitimate integration is extremely rare and a targeted chromosome duplication has not been reported. Here we systematically investigated the influence of design of the ends-out assay on the success of targeted genetic modification. We have determined transformation efficiency, fidelity of gene targeting and spectra of all aberrant events in several ends-out gene targeting assays designed to insert, delete or replace a particular sequence in the targeted region of the yeast genome. Furthermore, we have demonstrated for the first time that targeted chromosome duplications occur even during ends-in gene targeting. Most importantly, the whole chromosome duplication is *POL32* dependent pointing to break-induced replication (BIR) as the underlying mechanism. Moreover, the occurrence of duplication of the targeted chromosome was strikingly increased in the *exo1Δ sgs1Δ* double mutant but not in the respective single mutants demonstrating that the Exo1 and Sgs1 proteins independently suppress whole chromosome duplication during gene targeting.

1. Introduction

A linear DNA fragment introduced in the cell of the yeast *Saccharomyces cerevisiae* undergoes recombination with the homologous region in the genome (homologous recombination, HR). In order to perform gene targeting, yeast cells are transformed with a non-replicative DNA fragments carrying a selectable marker and containing ends homologous to the particular locus in the genome. These transforming DNA fragments are either (i) linear fragments used to replace the targeted sequence (gene replacement) [1] or (ii) linearized plasmids that integrate in the targeted locus (plasmid integration) [2,3]. Although both gene replacement and plasmid integration require proteins involved in HR [2–12], these two processes are mechanistically quite different [13]. After homologous pairing of the transforming DNA fragment and targeted sequence, the ends of the transforming DNA fragment point away from each other during gene replacement (ends-out gene targeting, EOGT) whereas during plasmid integration they point toward each other (ends-in gene targeting, EIGT).

In EIGT, the double-strand break (DSB) on the linearized plasmid is almost always repaired by HR resulting in targeted plasmid integration, whereas the frequency of random (non-targeted)

Abbreviations: HR, homologous recombination; EOGT, ends-out gene targeting; EIGT, ends-in gene targeting; DSB, double-strand break; TCD, targeted chromosome duplication; BIR, break-induced replication; bp, base pair; kb, kilobase; nt, nucleotide; PFGE, pulsed-field gel electrophoresis; ss, single stranded.

* Corresponding authors at: Laboratory for Biology and Microbial Genetics, Department of Biochemical Engineering, Faculty of Food Technology and Biotechnology, University of Zagreb, Pierottijeva 6, Zagreb 10000, Croatia.
Tel.: +385 1 483 6013; fax: +385 1 483 6016.
E-mail addresses: astafa@pbf.hr (A. Štafa), iksvetec@pbf.hr (I.-K. Svetec).
[1] Present address: Center for Proteomics, School of Medicine, University of Rijeka, Rijeka 51000, Croatia.

http://dx.doi.org/10.1016/j.dnarep.2014.07.004
1568-7864/

integration due to illegitimate recombination could be estimated to be as low as 0.1% [14]. Moreover, illegitimate integration, including homology-assisted illegitimate recombination [15,16] is the only aberrant event observed so far. Contrary to EIGT, the spectrum of aberrant events during EOGT is wider. Apart from (i) random integration by illegitimate recombination; transformation can result in (ii) integration of the transforming DNA fragment next to the homologous target, generating tandem repeats and (iii) targeted chromosome duplication (TCD) detected in aberrant transformants containing both, allele expected after a successful gene targeting and an untransformed allele (heteroallelic transformants) [14]. Duplication of a targeted chromosome can occur either by extensive DNA synthesis from the 3′-ends of the transforming fragment to the ends of the targeted chromosome by break-induced replication (BIR) [17,18] or by chromosome missegregation [19].

The fidelity of gene targeting and spectra of aberrant events during EOGT can be influenced by different parameters such as the length of the flanking homologies used for targeting [20–22] and GC content of the targeted region [23]. Although as few as 40 bp at each end ensures gene targeting, the success of targeted events increases with the length of flanking homologies [20–23]. Various studies using different eukaryotic model organisms suggest that the fidelity of EOGT is governed by the same rules. Transformation of the protozoa *Trypanosoma brucei* frequently occurs due to HR and fidelity of EOGT depends on the length of flanking homology [24–26]. A high fidelity of gene targeting (percentage of a successful gene targeting) has also been reported for the moss *Physcomitrella patens* [27,28]. Moreover, when flanking homologies are not of the same length, the transforming DNA fragment integrates next to the sequence sharing longer homology, frequently creating tandem repeats as previously reported in the moss [29], mouse cell lines [30] and yeast [14].

Gene targeting is managed by a number of proteins also involved in repair of chromosomal DSB by HR. DSB repair by HR starts by processing the DNA ends by 5′-3′ nuclease activity producing 3′-single stranded DNA tails. DNA resection is performed by several proteins including the MRX/Sae2 complex, Exo1 exonuclease, Sgs1 helicase and Dna2 endonuclease [31–33]. In the absence of Exo1 and Sgs1 only short 3′ single stranded DNA tails form and extensive resection is prevented. Exo1 is also involved in mismatch repair [34], survival of telomerase deficient cells [35] processing of the stalled replication forks [36] and its inactivation increases the frequency of gap repair and crossing over in the transformation assay [9]. Sgs1, a homolog of *Escherichia coli* RecQ helicase [37], functions in extensive resection of DNA ends and dissolves double Holliday junctions into non-crossovers [38,39]. Inactivation of the *SGS1* gene increases the efficiency of transformation in both EOGT and EIGT assay [12,40–42]. Langston and Symington [12] proposed that Sgs1 inhibits ends-out recombination not by heteroduplex rejection, as reported during single strand annealing [43], but by unwinding flanking sequences homologously paired with their genomic target. It has been shown that inactivation of both extensive DNA resection pathways, in the *exo1Δ sgs1Δ* double mutant, results in the increased transformation efficiency, using either the transforming DNA fragments for EOGT or chromosome fragments, presumably due to decreased degradation of the linear DNA [42,44]. Furthermore, the *exo1Δ sgs1Δ* double mutant shows an increased frequency of *de novo* telomere addition [42,44,45]. Therefore, inactivation of *EXO1* and *SGS1* genes could influence not only the efficiency of transformation [41,42] but also the fidelity of EOGT, as observed by Chung et al. [42], and spectrum of aberrant transformation events. Moreover, the proportion of all transformation outcomes, including targeted chromosome duplication, could be influenced by the design of the gene targeting assay.

DNA replication initiated at origins of replication during S-phase, as well as by BIR at DSBs, requires several DNA polymerases [reviewed in 46]. It has been shown that BIR is dependent on Pol32, a non-essential subunit of the Pol δ polymerase complex [47]. Therefore, the *pol32* mutation could be used to distinguish whether chromosome duplications observed during gene targeting occurs by BIR or chromosome missegregation.

In this study we followed transformation efficiency, fidelity of gene targeting and spectra of aberrant events in five EOGT and one EIGT assay. Heteroallelic transformants having both a transformed and an untransformed, targeted allele that arose due to TCD were ubiquitous aberrant events in all EOGT assays but, for the first time, they were also detected in the EIGT assay. We show that the appearance of TCD during EOGT is *POL32* dependent pointing to BIR as the underlying mechanism. Inactivation of *EXO1* and *SGS1* genes synergistically increased the transformation efficiency, during both EOGT and EIGT, as reported previously [41,42]. However, this effect was associated with a striking decrease in the fidelity of gene targeting due to increase of TCD. In addition, frequency of TCD was not increased in respective single mutants demonstrating that Exo1 and Sgs1 proteins independently suppress gene targeting-associated chromosome duplication.

2. Materials and methods

2.1. Plasmids and the transforming DNA fragments

All plasmids used for yeast transformation are constructed in this study. Plasmid pLUH is a derivate of pLS42 [48] carrying *LEU2*, *URA3* and *HIS3* genes and it was used as a circular replicative control in transformation experiments. All other non-replicative (integrative) plasmids used for generation of the DNA fragments for transformation are listed in Table 1. The pGU2 and pAGU2 plasmids differ only by the *RG* region, the central part of the *ARG4* gene (539 bp, EcoRV-Bsp1407I end-filled fragment) inserted in the NaeI site of the plasmid pGU2 backbone creating pAGU2. The plasmid pGU2 is a derivative of the pGEM-7ZF(−) (Promega) plasmid. It is constructed by deleting and end-filling EcoRI-HindIII fragment from the multiple cloning site (MCS) and Kpn2I-MluI region from the backbone. Resulting plasmid was used to create pGU2 by inserting the *URA3* fragment in the end-filled BamHI site. The *URA3* fragment was S1-treated 1638 bp EcoRI–EcoRI fragment from pCR2.1.TOPO-URA3 which was obtained by insertion of 1621 bp *URA3* PCR fragment (primers: ZG1 5′-gggaagacaagcaacgaaac-3′ and ZG4 5′-ttcattggttctggcgaggt-3′) in the plasmid pCR2.1.TOPO.

The plasmid pLGU+4 was constructed by inactivation of the NcoI site in the *URA3* gene by cutting and end-filling. Additionally, NcoI-MroI cut and end-filled *LEU2* PCR fragment (1815 bp, primers: YUPL5 5′-atataCCATGGcattatttttttcctcaacat-3′ and YDOL3 5′-atataTCCGGAgtgtttttattgttgtgtat-3′, containing NcoI and MroI sites, respectively) was inserted in the NaeI site of the plasmid backbone.

The pAUHI and pAULI plasmids were constructed by inserting the BamHI–BamHI end-filled *HIS3* gene (1771 bp) and NcoI-MroI end-filled *LEU2* gene (1815 bp) in the StuI site in the *URA3* gene of the plasmid pAGU2, respectively. The plasmid pADULI was constructed by replacing the StuI-EcoRV fragment from the *URA3* gene (248 bp) of the plasmid pAGU2 with the NcoI-MroI end-filled *LEU2* gene (1815 bp).

Plasmid pAGUS was constructed by replacing PvuII-PvuII fragment (2038 bp) containing 1638 bp *URA3* region of the plasmid pAGU2 with the SmaI–SmaI fragment (1104 bp) carrying shorter *URA3* region from the plasmid pTZGU [14]. Standard media and procedures were used for the cultivation of the *E. coli* strains (DH5α and XL1blue) and DNA manipulations [49].

Table 1
Plasmids carrying DNA fragments used either for a strain construction or as the transforming DNA fragments in gene targeting assays. Alleles used in EOGT assays are shown in bold. *RG* region denotes the central part of the *ARG4* gene.

Plasmid	Contains yeast regions	Use
pGU2	• *URA3*	Construction of strains used in EOGT assays 1 and 2 (Fig. 1A)
pLGU + 4[a]	• *ura3::NcoI*: *URA3* gene inactivated by end-filling of the NcoI site, • *LEU2*: fragment inserted in the NaeI site of the plasmid backbone	Construction of strain used in EOGT ends-out assay 4 (Fig. 1A)
pAGU2	• *URA3*, • *RG:* central part of *ARG4* gene inserted in the NaeI site of the plasmid backbone	Generation of the transforming DNA fragment used in EOGT assays 4 and 5 (Fig. 1A)
pAUHI[b]	• *ura3::HIS3: HIS3* gene (1771 bp) inserted in the StuI site within the *URA3* gene, • *RG*	Construction of strains used in EOGT assays 3 and 5 (Fig. 1A)
pAULI[b]	• *ura3::LEU2*: *LEU2* gene (1815 bp) inserted in the StuI site within the *URA3* gene, • *RG*	Generation of the transforming DNA fragment used in EOGT assays 1 and 3 (Fig. 1A)
pADULI[b]	• *ura3Δ::LEU2*: EcoRV-StuI region (248 bp) within the *URA3* gene is replaced with *LEU2* gene (1815 bp), • *RG*	Generation of the transforming DNA fragment used in EOGT assay 2 (Fig. 1A)
pAGUS[b]	• *URA3*: shorter *URA3* region replaces PvuII–PvuII region of pAGU2, • *RG*	The transforming DNA fragment used in EIGT assay (Fig. 2A) after linearization with SacI within *RG* region

[a] pGU2 derivates.
[b] pAGU2 derivates.

2.2. Yeast strains

S. cerevisiae strains used in this study are derivatives of BY4741 and BY4742 [50] and are listed in Table 2. All modifications of the *URA3* region in different strains were made using the plasmids listed in Table 1. Haploid α-mating type strains were transformed with the transforming DNA fragment carrying specific *URA3* allele and successful modification was confirmed by Southern blotting. Strains were mated with a-mating type strain and dissected, using only a-mating type haploids in further experiments.

The yeast strain BYαURA3 was constructed by transforming the strain BY4742 with EcoRI–EcoRI fragment carrying *URA3* region from pGU2 (1638 bp). The strain BYaURA3 was constructed by crossing BYαURA3 with the strain BY4741, followed by sporulation and dissection. The strain BYauN was constructed by the integration of the StuI linearized plasmid pLGU + 4 in the *URA3* region of the strain BYaURA3 and subsequent loss of integrated plasmid resulting in cells with *ura3::NcoI* allele that grow on 5-FOA. Transformation of the strain BYaURA3 with XhoI-SmaI fragment carrying *ura3::HIS3* allele (3298 bp) resulted in the construction of the yeast strain BYauH.

Strain Y11809 (*exo1Δ*) was crossed with BY4742 followed by dissection thus constructing haploid strain BYa *exo1Δ*. Strains BYauH *exo1Δ*, BYαuH *exo1Δ* and BYauH *sgs1Δ* were constructed by crossing strain BYauH with the strains Y11809 (*exo1Δ*) or Y10775 (*sgs1Δ*) and dissection. Haploid yeast strain BYa *exo1Δ sgs1Δ* was constructed by crossing strains BYa *exo1Δ* with single mutant Y10775 (*sgs1Δ*) and dissection while the strain BYauH *exo1Δ sgs1Δ* was constructed by crossing BYαuH *exo1Δ* and BYauH *sgs1Δ* followed by dissection. The strain BYaU *exo1Δ sgs1Δ* was constructed by transforming the strain BYauH *exo1Δ sgs1Δ* with *URA3* region from the pGU2 plasmid, selection of Ura^+ His^- transformants followed by Southern blot analysis. Since both *SGS1* and *EXO1* genes were disrupted by *kanMX4* cassette, the presence of two disruption cassettes in the *exo1Δ sgs1Δ* double mutant was confirmed by Southern blotting. BYauH *pol32Δ* was constructed by transforming BYauH with *pol32Δ::kanMX4* cassette amplified by PCR using primers *pol32*-F (5′-aattctcgatcagtatgcctcaata-3′) and *pol32*-R (5′-cctgtacccaattttccttttagat-3′) and the disruption was confirmed by PCR. Throughout the work, standard methods for yeast growth and manipulation were used [51].

2.3. Transformation assays

In gene targeting assays presented in Figs. 1A and 2A, yeast transformation was done using the lithium acetate procedure

Table 2
Yeast strains used in this study.

Strain name	Genotype	Reference
BY4741	*MATa his3Δ1 leu2Δ0 met15Δ0 ura3Δ0*	[50]
BY4742	*MATα his3Δ1 leu2Δ0 lys2Δ0 ura3Δ0*	[50]
Y11809	*MATα his3Δ1 leu2Δ0 lys2Δ0 ura3Δ0 exo1::kanMX4*	EUROSCARF
Y10775	*MATα his3Δ1 leu2Δ0 lys2Δ0 ura3Δ0 sgs1::kanMX4*	EUROSCARF
BYαURA3	*MATα his3Δ1 leu2Δ0 lys2Δ0 URA3*	This study
BYaURA3	*MATa his3Δ1 leu2Δ0 met15Δ0 URA3*	This study
BYauN	*MATa his3Δ1 leu2Δ0 lys2Δ0 ura3::NcoI*	This study
BYauH	*MATa his3Δ1 leu2Δ0 met15Δ0 ura3::HIS3*	This study
BYa *exo1Δ*	*MATa his3Δ1 leu2Δ0 met15Δ0 ura3Δ0 exo1::kanMX4*	This study
BYauH *exo1Δ*	*MATa his3Δ1 leu2Δ0 met15Δ0 ura3::HIS3 exo1::kanMX4*	This study
BYαuH *exo1Δ*	*MATα his3Δ1 leu2Δ0 lys2Δ0 ura3::HIS3 exo1::kanMX4*	This study
BYauH *sgs1Δ*	*MATa his3Δ1 leu2Δ0 met15Δ0 ura3::HIS3 sgs1::kanMX4*	This study
BYa *exo1Δ sgs1Δ*	*MATa his3Δ1 leu2Δ0 met15Δ0 ura3Δ0 exo1::kanMX4 sgs1::kanMX4*	This study
BYaU *exo1Δ sgs1Δ*	*MATa his3Δ1 leu2Δ0 met15Δ0 exo1::kanMX4 sgs1::kanMX4*	This study
BYauH *exo1Δ sgs1Δ*	*MATa his3Δ1 leu2Δ0 met15Δ0 ura3::HIS3 exo1::kanMX4 sgs1::kanMX4*	This study
BYauH *pol32Δ*	*MATa his3Δ1 leu2Δ0 met15Δ0 ura3::HIS3 pol32::kanMX4*	This study

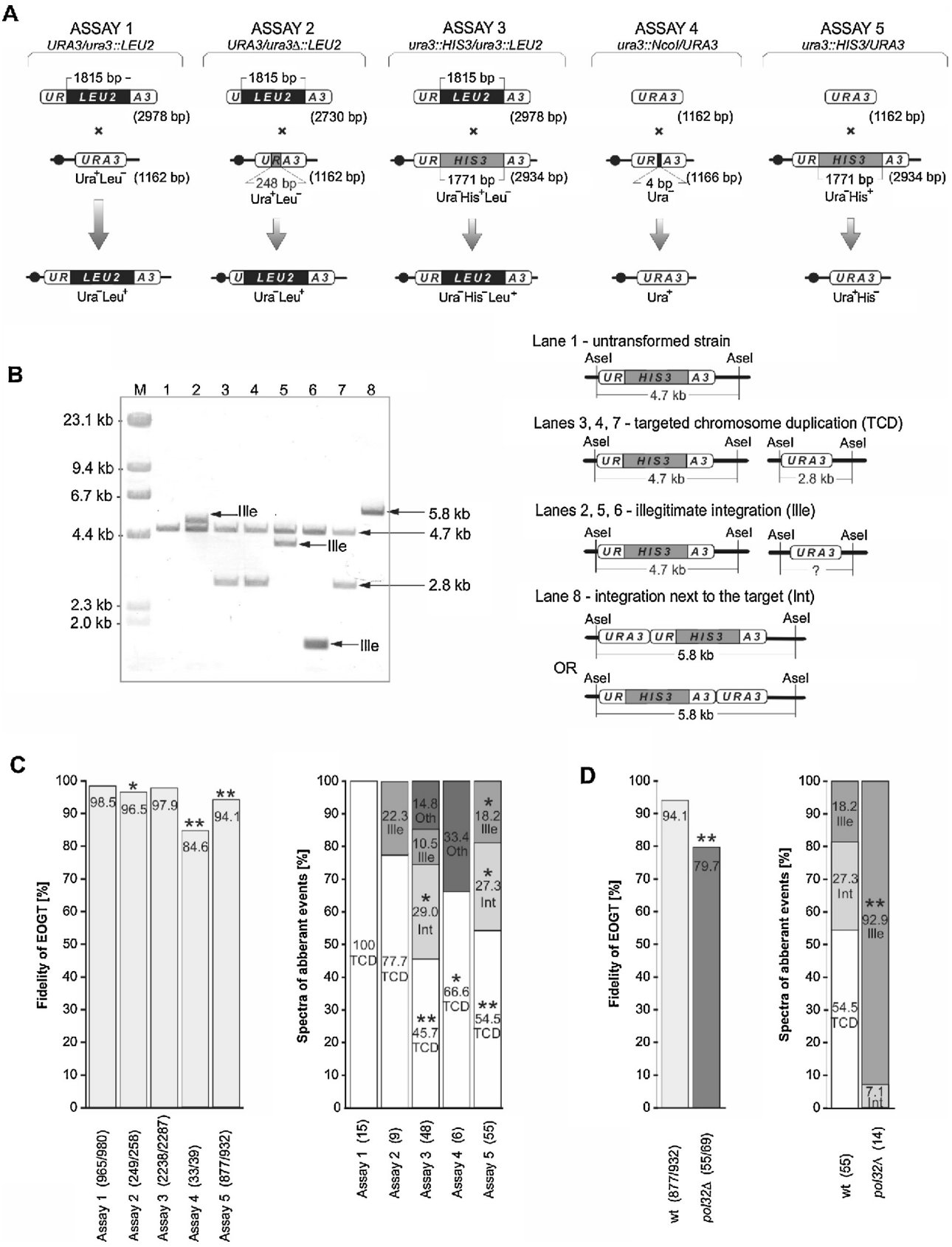

Fig. 1. Ends-out gene targeting (EOGT) experimental system and results. (A) EOGT assays designed to insert (assay 1), replace (assays 2 and 3) and delete (assays 4 and 5) particular sequence in *URA3* region on the chromosome V. In each assay, the transforming DNA fragment, targeted region and outcome of successful gene targeting are shown. The overall length of transforming and targeted DNA is indicated in parentheses. (B) Typical result of Southern blot analysis and schematic explanation of the aberrant transformants obtained in assay 5. Genomic DNA was cut with AseI and hybridized to the labeled *URA3* gene. M-DNA of bacteriophage λ cut with HindIII, lane 1 untransformed strain; lines 2–8 aberrant Ura$^+$ His$^+$ transformants. (C) Fidelity of EOGT and spectra of aberrant events in five assays for wild type and (D) in the assay 5 for *pol32Δ* mutant. Numbers of transformants analyzed are indicated in parenthesis, Oth represent other uncharacterized or complex aberrant events, *p* values of significant differences compared to results from (C) assay 1 or (D) wild type are highlighted by the asterisks ($^*p < 0.05$, $^{**}p \leq 0.0001$).

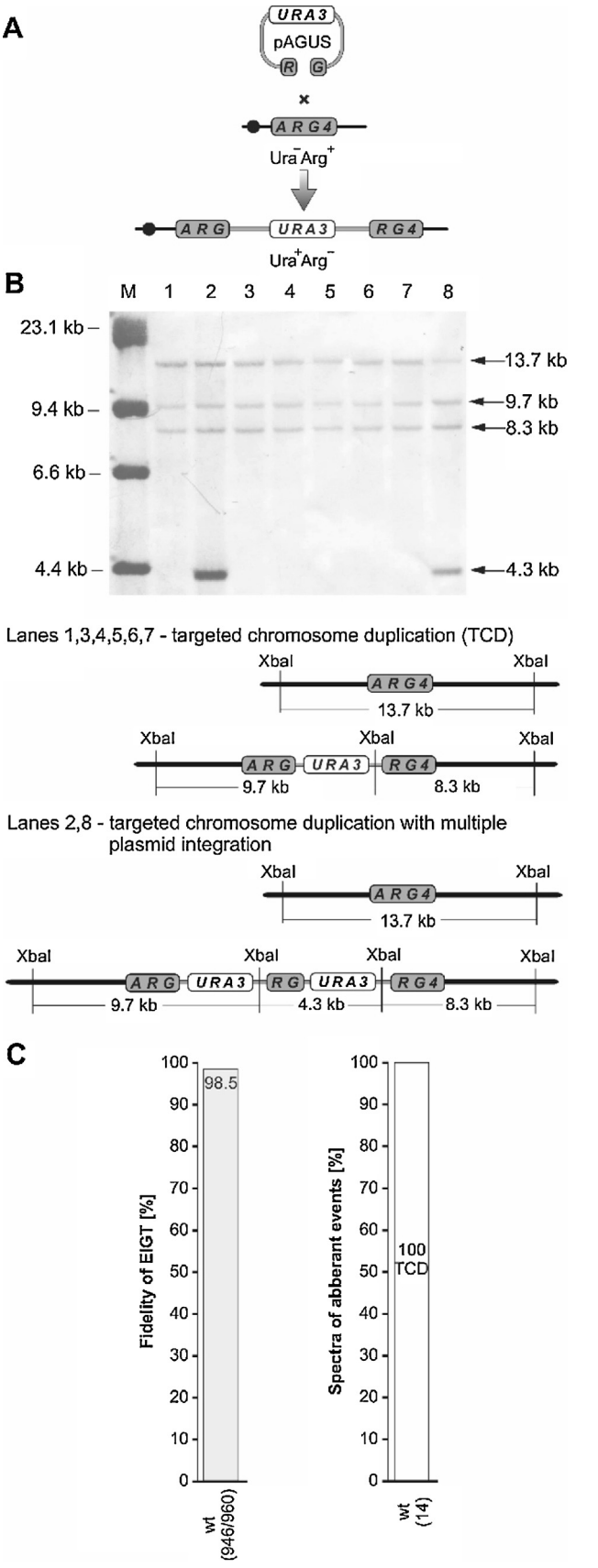

Fig. 2. Ends-in gene targeting (EIGT) experimental system and results. (A) EIGT assay designed to disrupt *ARG4* gene on the chromosome VIII. Linearized plasmid pAGUS, targeted region and successful gene targeting outcome are shown. (B) Typical result of Southern blot analysis and schematic explanation of the aberrant transformants obtained in EIGT assay. Genomic DNA was cut with XbaI and hybridized to the labeled *ARG4* gene. M-DNA of bacteriophage λ cut with HindIII, lanes 1–8 aberrant Arg⁺ Ura⁺ transformants. (C) Fidelity of EIGT and spectra of aberrant events in wild type. Numbers of transformants analyzed are indicated in parenthesis.

omitting carrier DNA [52]. One isolate per strain in wild type and single mutants and two isolates from *exo1Δ sgs1Δ* background were tested. Transformations were performed in duplicate using the same transforming DNA fragment and batch of cells, and each assay was carried out at least three independent times, transformants obtained in each assay were pooled for analysis.

2.3.1. Spectra of transformation events in ends-out gene targeting (EOGT)

In EOGT assays (Fig. 1A), corresponding yeast strains were transformed with 500 ng of the transforming DNA fragment generated by cutting the plasmids pAULI (assays 1 and 3), pADULI (assay 2) and pAGU2 (assays 4 and 5) with HindIII and isolated from the agarose gel (Table 1). To determine the fidelity of EOGT (proportion of targeted events) and spectra of aberrant transformation events in each assay, transformants were first analyzed by replica plating. In assays 1–3 and 4–5, transformants were selected on SC-leu and SC-ura plates, respectively, followed by replica plating to select for transformants with aberrant phenotype (for assays 1–2 Leu⁺ Ura⁺; assay 3 Leu⁺ His⁺, assay 5 Ura⁺ His⁺). Aberrant phenotype was determined for 15/980 (assay 1), 9/258 (assay 2), 48/2287 (assay 3), 6/39 (assay 4) and 55/932 (assay 5) transformants in wild type. In assay 5, 11/395 transformants from *exo1* mutant, 7/190 from *sgs1*, 1431/1451 from *exo1 sgs1* double mutant and 14/69 from *pol32* background had an aberrant phenotype. Spectra of the transformation events in all transformants with the aberrant phenotype were determined by Southern blotting (Figs. S1–S3). Since assay 4 did not allow phenotypic distinction of targeted and aberrant transformation outcomes, all transformants were analyzed by Southern blotting (Fig. S3). 2–3 representative transformants for each assay, shown by Southern blotting to contain both an untransformed and region after gene targeting (heteroallelic transformants), were further analyzed by pulsed-field gel electrophoresis (PFGE, Fig. S4) [14] and flow cytometry (2.5) to confirm TCD and DNA content. In the assay 5, due to the significant increase of the percentage of the aberrant transformation events, 75 of aberrant transformants from the *exo1Δ sgs1Δ* double mutant were analyzed by Southern blotting, 7 transformants that contained both the untransformed and gene targeting allele were further analyzed by whole chromosome PFGE (Fig. 3) and 2 of them were analyzed by flow cytometry (2.5).

2.3.2. Spectra of transformation events in ends-in gene targeting (EIGT)

In EIGT assay (Fig. 2A), strains BY4741 and BYa *exo1Δ sgs1Δ* were transformed with 200 ng of plasmid pAGUS linearized with SacI within *RG* region (539 bp central part of the *ARG4* gene) and isolated from the agarose gel. In this assay, half of the transformation mixture was plated on SC-ura to allow growth of all transformants (Ura⁺ phenotype) while the other half was plated on SC-ura-arg to select for aberrant transformants only (Ura⁺ Arg⁺ phenotype). In wild type 14/960 while in the double *exo1Δ sgs1Δ* mutant 482/498 transformants had an aberrant phenotype. As in ends-out assays, all transformants with the aberrant phenotype from the wild type (14) and 40 from the *exo1Δ sgs1Δ* double mutant were analyzed by Southern blotting, 6 of them by whole chromosome PFGE or PFGE of SacII cut plugs (Fig. S5) and 2 by flow cytometry (2.5).

2.3.3. Transformation efficiency

In order to determine transformation efficiency in DNA repair mutants (Fig. 3A) yeast strains were transformed either with 1000 ng of the plasmid DNA (pAULI or pAGU2) cut with HindIII

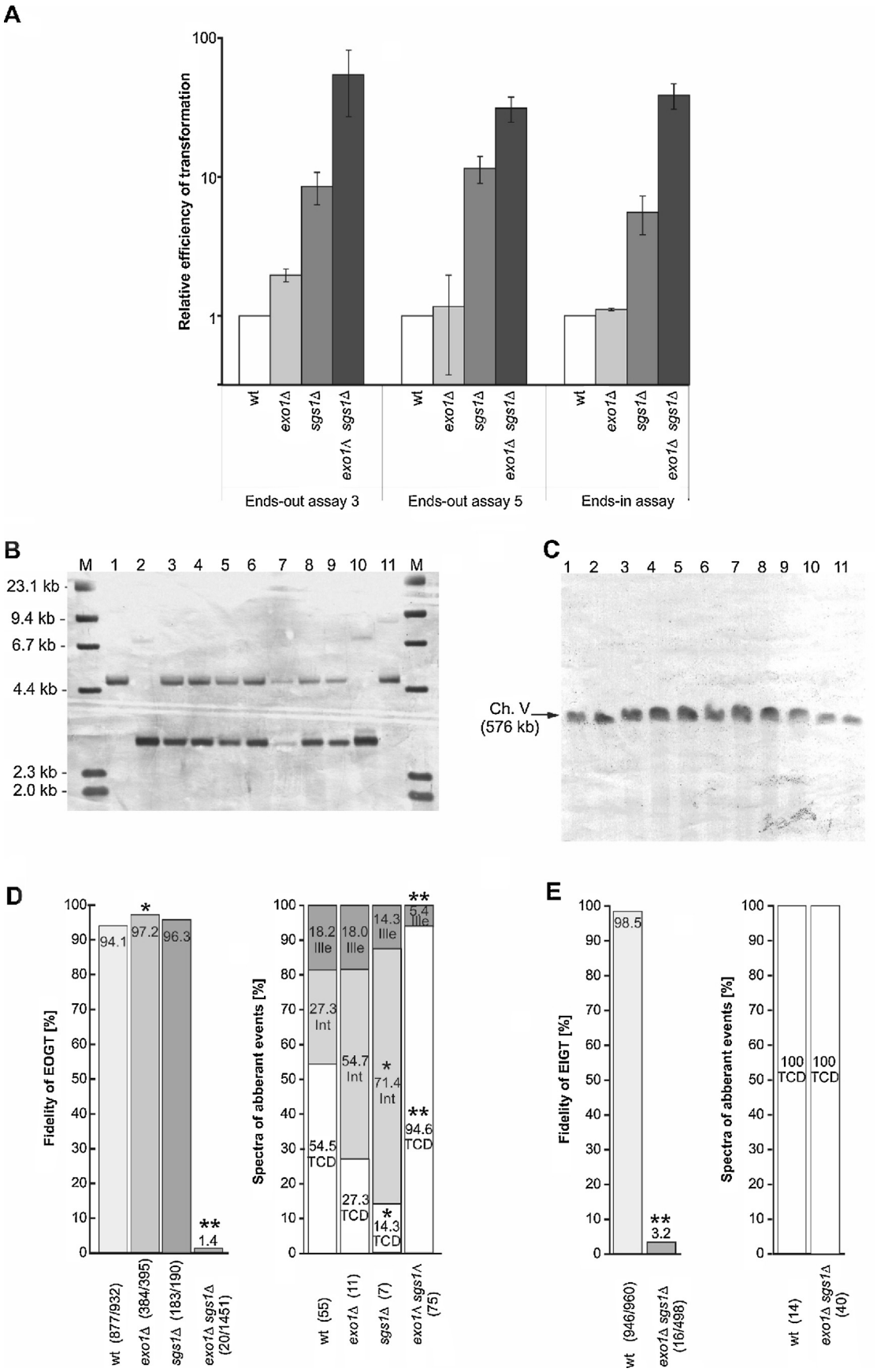

Fig. 3. Transformation efficiency and the spectra of transformation events in EOGT and EIGT assays for the *exo1Δ* and *sgs1Δ* single mutants and the *exo1Δ sgs1Δ* double mutant. (A) Relative efficiency of transformation is expressed as the ratio of the number of transformants obtained in a specific assay (EOGT assays 3 and 5 and EIGT assay) and with replicative plasmid pLUH and then normalized to wild type. (B) Genomic DNA of the aberrant transformants from the double *exo1Δ sgs1Δ* mutant in assay 5 was

(EOGT assays 3 and 5) or 100 ng of the plasmid pAGUS linearized within *RG* region with SacI (EIGT assay). To allow the comparison of results from different strains, relative efficiency of transformation was expressed as the ratio of the number of transformants obtained in each assay and with 100 ng of the circular replicative plasmid pLUH.

2.4. Molecular analysis of the transformants

Southern blot and PFGE analysis of genomic DNA were described previously [14,53]. Conditions for whole chromosome PFGE of wild type transformants were as follows: 0.5× TBE, 1% agarose, 6 V/cm, 24 h, switch time 60–120 s, or in the case of transformants from the *exo1Δ sgs1Δ* double mutant switch time was changed to 24–205 s. Conditions for separation of DNA fragments from SacII cut plugs were: 0.5× TBE, 1% agarose, 6 V/cm, 11 h, switch time 1–6 s. Molecular analysis was done using DIG-labeled PCR amplified *URA3* (primers ZG1 and ZG4), *kanMX* (primers *Kan*Up 5′-aaaaaataggcgtatcacgag-3′ and *Kan*Dn 5′-tcgatgataagctgtcaaac-3′) or *ARG4* probe (primers *ARG4*-F 5′-taacgtcgccatctgctaa-3′ i *ARG4*-R 5′-catgtcagacggcactcaa-3′).

2.5. Flow cytometry

Determination of DNA content by flow cytometry was done using protocol previously described by Gerstein et al. [54] and analyzed by Accuri-6 (Accuri Cytometrics Inc.). For each transformant two independent cell preparations were analyzed and the DNA content was calculated with respect to the non-transformed parental haploid and diploid strains.

2.6. Statistical analysis

Statistical significance was determined after pooling transformants from several independent transformations using two-tailed Pearson's Chi-squared test (χ^2; http://in-silico.net/). When gene targeting fidelity was compared between different assays, numbers of transformants due to a successful gene targeting were compared to those from assay 1, or results from mutant strains were compared to wild type results from assay 5 (Figs. 1C and D, 2C, 3D and E; *e.g.* 249 gene targeting transformants/258 total transformants from assay 2 were compared to 965 gene targeting/980 transformants from assay 1). Statistical significance of spectra of aberrant genetic events was determined by comparing number of transformants due to a specific type of an aberrant event among all aberrant transformants with results from assay 1 or for mutants to wild type assay 5 results (*e.g.* 6 TCD events/9 aberrant transformants from assay 2 were compared to 15 TCD events/15 aberrant transformants from assay 1).

3. Results

Ends-out gene targeting (EOGT) is usually used to replace a particular endogenous sequence with the one on the transforming DNA fragment although this approach could also be used to insert or delete various sized sequences from the targeted locus. On the other hand, ends-in gene targeting (EIGT) is used to insert the transforming DNA, most frequently linearized plasmid, into a particular position of the genome. The main aims of this study were to determine the fidelity of gene targeting and the spectra of aberrant transformation outcomes in specific EOGT assays as well as to investigate if targeted chromosome duplication (TCD) occurs during EIGT. To accomplish this, we employed five different EOGT assays (Fig. 1A) and one EIGT assay (Fig. 2A). EOGT assay 1 was designed to insert 1.81 kb (*LEU2* gene) in the targeted locus; in assays 2 and 3 the expected outcomes were replacement of 0.25 kb and 1.77 kb (*HIS3* gene) sequences with the *LEU2* gene; whereas in assays 4 and 5, 4 bp and a 1.77 kb (*HIS3* gene) were deleted from the targeted locus, respectively. Additionally, EIGT assay (Fig. 2A) allowed us to select for aberrant transformation outcomes during plasmid integration.

3.1. Transformation efficiencies in EOGT assays

To investigate if the fidelity of EOGT depends on the type of intended genome modification we used 5 specific assays (Fig. 1A). Lengths of the upstream and downstream flanking homologies on the transforming DNA fragment in most assays were the same (0.66 kb and 0.50 kb, respectively). Exceptions to this were in assay 2 (carrying 0.41 kb and 0.50 kb upstream and downstream homology, respectively) and assay 4 (with 0.43 kb and 0.73 kb of upstream and downstream homology, respectively). Since flanking homologies were of comparable sizes and significantly above minimal efficient processing segment (MEPS) we expected that the resulting transformation efficiencies were influenced by the design (specificity) of each transformation assay, such as the length of inserted, replaced or deleted sequence from the targeted locus. Although transformation efficiency varied only 3-fold among assays 1 and 5 (Fig. S6), it was slightly higher for the insertion assay (1) than for replacement assays (2 and 3), decreasing further in deletion assay (5), consistent with the results of molecular analysis of transformants (see Section 3.2).

3.2. Fidelity of EOGT in wild type

To determine the fidelity of EOGT (proportion of targeted events) and the spectra of aberrant events in five ends-out assays (Fig. 1A), transformants obtained in each assay were analyzed as described in Section 2.3.1. The typical Southern blot analysis and the schematic explanation of the aberrant transformants are shown in Figs. 1B and S1–S4.

The fidelity of EOGT was high in all assays in the wild type, ranging from 84.61% to 98.47% (33/39 for assay 4 to 965/980 for assay 1, Fig. 1C). However, consistent with the transformation efficiency results (Fig S6), the proportion of successful gene targeting was slightly higher for the insertion (assay 1; 965/980 transformants analyzed, 98.47%), replacement assay 2 (249/258, 96.51%) and assay 3 (2238/2287 transformants, 97.86%, $p = 0.0424$ and $p = 0.2785$ for assay 2 and 3 compared to assay 1, respectively) than for the deletion assay 5 (877/932 transformants, 94.10% of gene targeting, $p < 0.0001$ compared to assay 1). Moreover, when a longer DNA sequence was inserted, replaced or deleted (assays 1–3 and 5) the fidelity of gene targeting was significantly higher compared to the deletion of only 4 bp from the genome (33/39; 84.62%, $p < 0.0001$ compared to assay 1) further reinforcing that design of the experimental system *per se* influences the fidelity of gene targeting. Lower gene targeting fidelity in assay 4 could be explained by the involvement of mismatch repair in the recognition of 4 bp heterologous sequence from NcoI end-filled site in the *URA3* gene [55].

cut with AseI and (C) PFGE analysis of whole chromosomes of the same samples. Lanes 1 and 11 untransformed *ura3::HIS3* strain (His$^+$ Ura$^-$ phenotype), lanes 2 and 10 gene targeting transformants with *URA3* allele (His$^-$ Ura$^+$ phenotype), lanes 3–9 transformants with the aberrant His$^+$ Ura$^+$ phenotype containing both *ura3::HIS3* and *URA3* alleles, DNA was hybridized to the labeled *URA3* gene. (D) Fidelity of EOGT and spectra of aberrant events in assay 5 and (E) fidelity of EIGT and spectra of aberrant events in selected mutants. Error bars represent standard deviations, numbers of transformants analyzed are indicated in parenthesis, *p* values of significant differences compared to wild type strain are highlighted by the asterisks ($^*p < 0.05$, $^{**}p \leq 0.0001$).

Aberrant transformation events obtained in EOGT include (i) heteroallelic transformants having two copies of a targeted chromosome (ii) integration of the transforming DNA fragment next to the targeted region and (iii) illegitimate integration (Figs. 1B and S1–S4). Both heteroallelic transformants and integration of the targeted DNA fragment next to the targeted region have already been described in detail in an EOGT assay designed to delete the 6.1 kb *Ty1* retrotransposon from the *ura3-52* allele [14].

The spectra of aberrant events described here (Fig. 1C) clearly shows that, even in wild type, TCD is the dominant class of all aberrant events ranging from 22/48 aberrant transformants in EOGT assay 3 (45.74%) to 15 TCDs of 15 aberrant transformants in assay 1 (100.00%). Integration of the transforming DNA next to the targeted locus was observed only in assay 3 (14/48 aberrant events, 29.06%) and in assay 5 (15/55 aberrant events, 27.27%, $p = 0.003$ and $p = 0.004$ for assays 3 and 5, compared to 0/15 in assay 1, respectively) where the transforming DNA fragment had either the same length or it was shorter than the targeted sequence, suggesting they occur as a consequence of the hindered ability of the transforming DNA fragment to simultaneously invade both flanking homologies in the genome. This observation is in accordance with the proposed model for single and multiple integration of ends-out transforming fragment next to the targeted sequence [14].

3.3. Fidelity of EOGT in pol32 background

It has been shown that a chromosomal DSB can promote chromosome missegregation during mitosis yielding one nullsomic and one disomic cell [19]. Moreover, we have proposed previously that EOGT can promote TCD either due to BIR or non-disjunction of sister chromatids [14]. To reveal the mechanism underlying TCD, we determined the spectrum of transformation events for EOGT assay 5 in the *pol32Δ* mutant that is impaired for BIR (Figs. 1A and D). Although the fidelity of EOGT was significantly lower than in wild type with 55/69 gene targeting events (79.71%) compared to 877/932 in wild type (94.10%; $p < 0.0001$), TCDs were abolished (0/14 compared to 30/55 aberrant events in wild type, $p = 0.0002$) confirming they are a consequence of BIR. The observed significant increase in aberrant events was due to illegitimate integration (13/14 compared to 10/55 in wild type, $p < 0.0001$).

3.4. Transformation efficiency and fidelity of EOGT in the exo1 and sgs1 single and the exo1 sgs1 double mutants

Inactivation of both *EXO1* and *SGS1* genes influences the stability of the transforming DNA fragment resulting in an increased efficiency of transformation [41,42,44]. Therefore, we suspected it might also influence the fidelity of EOGT and the spectrum of transformation events. The efficiency of transformation for the *exo1Δ* and *sgs1Δ* single and the *exo1Δ sgs1Δ* double mutants in EOGT assays 3 and 5 was determined (Fig. 3A). While deletion of the *EXO1* gene had only minor effect on the efficiency of transformation, the inactivation of *SGS1* gene resulted in 8.5-fold and 11.5-fold increase in EOGT assays 3 and 5, respectively. At the same time, inactivation of both genes increased the efficiency of transformation in assays 3 and 5 by 54.4-fold and 31.2-fold, respectively (Fig. 3A).

The influence of *exo1Δ* and *sgs1Δ* mutations on fidelity of gene targeting was analyzed in assay 5 (Figs. 3B–D). While the *exo1Δ* mutant displayed slightly higher fidelity of EOGT compared to the wild type (384/395 transformants compared to 877/932, $p = 0.0118$), the *sgs1Δ* mutant was similar to the wild type (183/190 compared to 877/932, $p = 0.2007$). A striking shift toward the aberrant events was observed in the *exo1Δ sgs1Δ* double mutant compared to wild type, with 98.62% of all transformants being aberrant (20 gene targeting events of 1451 transformants analyzed, compared to 877/932 in wild type, $p < 0.0001$). Moreover, 71 of 75 (94.62%) aberrant transformants analyzed in the *exo1Δ sgs1Δ* double mutant had TCD, compared to 30 of 55 (54.55%) in wild type ($p < 0.0001$; Fig. 3B–D) and analysis of 2 aberrant TCD transformants confirmed they had haploid DNA content (1.09 and 1.16). To confirm the generality of these results, the percentage of aberrant transformation events in the *exo1Δ sgs1Δ* double mutant for assays 1 and 2 was determined by replica plating (98.5% and 97.73%, respectfully). Therefore, we suggest that due to the inactivation of both extensive resection pathways, the transforming DNA fragment becomes stabilized and engages more frequently in BIR. We could not directly test this hypothesis due to lethality of the *pol32Δ sgs1Δ* double mutant [56].

3.5. Fidelity of EIGT in wild type and the exo1 sgs1 double mutant

As reported by others and here, deletion of *EXO1* and *SGS1* genes synergistically increased the transformation efficiency in both EOGT and EIGT [41,42] (Fig. 3A). In the EOGT assays described here, this increase coincides with the striking increase in the proportion of aberrant events, more precisely an increase in TCD (Figs. 3B–D). Therefore, we used an EIGT assay that allows phenotypic distinction between targeted and aberrant transformation events (Figs. 2A and B). In this assay, targeted plasmid integration results in the disruption of endogenous *ARG4* gene and Arg^- Ura^+ phenotype, whereas aberrant events result in an Arg^+ Ura^+ phenotype. Since we expected an extremely low proportion of aberrant events in wild type, the fidelity of gene targeting was determined not only by replica plating but also by direct selection of aberrant transformants; one half of the transformation mixture was plated on SC-ura to select for all types of transformation events (both targeted plasmid integration and aberrant events) and the other half on SC-ura-arg plates, to select for aberrant events only. The proportion of Ura^+ Arg^- transformants due to gene targeting was 98.54% (946/960) and Southern blot analysis revealed that all aberrant transformants from the wild type (14/14) were heteroallelic (Fig. 2C).

The percentage of transformants with the aberrant Arg^+ Ura^+ phenotype increased to 96.82% (482/498) in the *exo1Δ sgs1Δ* double mutant ($p < 0.0001$). It was confirmed by Southern blotting that all analyzed aberrant transformants (40/40) were heteroallelic, containing both an intact *ARG4* locus and *arg4* disrupted by plasmid integration (Fig. S5A). Furthermore, PFGE analysis of 6 heteroallelic transformants showed hybridization only to the chromosome VIII (Fig. S5B) while flow cytometry analysis of two transformants with aberrant phenotype revealed haploid DNA content. Additionally, results of restriction analysis of PFGE plugs with SacII (Fig. S5C) again revealed the existence of two alleles: one contained untransformed *ARG4* allele (35 kb band) while the other was due to either single or multiple plasmid integration in the *ARG4* region (plasmid integration band 39.3 kb), confirming that heteroallelic transformants arose due to TCD. These results are in accordance with the results obtained in EOGT, showing that Exo1 and Sgs1 proteins contribute to the suppression of gene targeting-associated chromosome duplications.

4. Discussion

S. cerevisiae is a model eukaryotic organism with extremely efficient HR and high fidelity of gene targeting [22,57]. Proteins involved in DSB repair by HR in yeast have their functional, and even structural homologues in higher eukaryotes and plants, suggesting that the same rules might govern gene targeting and giving hope for improving gene targeting and gene therapy as well [58–67]. One of the major problems associated with gene targeting in all higher eukaryotes are mistargeted events [28,68–72]. We had shown

previously that mistargeted events occur during EOGT even in *S. cerevisiae* [14]. These events include: illegitimate integration, integration of the transforming DNA next to the target sequence and TCD. As a continuation of our studies, we have developed several EOGT and one EIGT assay and here we show that gene targeting success is influenced not only by the length of flanking homologies, but also by the type of intended genome modification by EOGT and the overall length of the transforming DNA fragment with the respect to the targeted sequence in the genome.

4.1. Fidelity of EOGT depends on the type of intended genome modification

Successful EOGT requires flanking homologies at the ends of the transforming DNA fragment to target it to the particular region in the genome. Although throughout the literature gene targeting by ends-out recombination is frequently called gene replacement, here we describe five EOGT assays (Fig. 1A), used to modify the targeted region in the yeast genome, distinguishing between insertion (assay 1), replacement (assays 2 and 3) and deletion (assays 4 and 5). All the transforming DNA fragments, used in EOGT assays, had flanking homologies above 0.41 kb. Therefore, we might expect that the observed differences in the spectra of transformation events depended on the type of intended genome modification by EOGT, length ratio of the transforming and targeted sequence and heteroduplex structure formed during recombination.

A large number of transformants analyzed for each assay, allowed us to draw several important conclusions and to hypothesize about causes of the observed effects. Although the differences in the fidelity of gene targeting between EOGT assays were small (84.61–98.47%), most of them are statistically significant (see Sections 3.2–3.4, Fig. 1C). Insertion assay 1 showed the highest (98.5%) while deletion assays (4 and 5) had the lowest fidelity of EOGT (84.6% and 94.1%), confirming that even in yeast it is easier to insert than to delete a sequence in the genome, as has been previously observed for gene targeting in human cell culture [73]. Replacement assays (2 and 3), mimic the experimental design used in most laboratories for the construction of knock-out strains during which a part, or the entire ORF, is replaced with selectable marker and both resulted in intermediate targeting fidelity (96.5% and 97.9%).

We were not able to distinguish whether gene targeting occurs by assimilation of a single stranded DNA [10] or by two independent strand invasions [11,12]. However, we hypothesize that a single strand of the transforming DNA fragment can be assimilated in the recipient DNA if it is entirely homologous to the target sequence, more precisely if it does not contain any sequence heterologous to the targeted locus (EOGT assays 4 and 5). On the other hand, if the transforming DNA fragment contains heterologous insertion (EOGT assays 1–3), single stranded DNA cannot be entirely assimilated so gene targeting is a consequence of two independent strand invasions [11,12].

The lowest fidelity of EOGT achieved in ends-out assay 4 (84.6% *vs.* 98.5%, Fig. 1C) is rather a consequence of an interaction between the transforming and the targeted DNA than property of the transforming DNA fragment *per se* because the use of the same DNA fragment in assay 5 resulted in higher EOGT fidelity. In both assays (4 and 5) the transforming DNA fragment does not contain a heterologous insertion and therefore can undergo single stranded DNA assimilation. However, assimilation of a single strand of the transforming DNA in assay 4 results in formation of heteroduplex DNA containing 4 nucleotide (nt) single stranded loop and it was already shown that short heterologies (up to 14 bp) recognized by mismatch repair proteins [55] are more anti-recombinogenic than the large ones [74–76] such as those that could appear in assay 5. Therefore, efficient single stranded DNA assimilation in the recombination intermediate, followed by a strong antirecombinogenic effect of 4 bp heterology could result in the frequent displacement of the assimilated single stranded DNA and an appearance of a single stranded transforming DNA fragment. This is in agreement with the previous reports showing that single stranded DNA is highly recombinogenic, being less affected by antirecombinogenic effect of point mutations [77], prone to illegitimate recombination and able to induce genome rearrangement [53].

The lower fidelity of EOGT in assay 5, compared to assay 1 (94.1 5 *vs.* 98.5%, Fig. 1C), could be a consequence of several phenomena. First, it is possible that it is easier to insert than to delete sequence from the genome because genome-borne insertion has a stronger anti-recombinogenic effect than the insertion present on the transforming DNA. Second, if formed in heteroduplex, large single stranded loops are preferentially repaired using a genomic DNA as a template. However, it is also possible that fidelity of gene targeting is influenced by the length ratio between transforming DNA and targeted region. This hypothesis is supported by the fact that in assay 5 the transforming DNA is significantly shorter than targeted region in the genome (1.16 kb *vs.* 2.93 kb, respectively) hindering simultaneous invasion of both ends of transforming DNA in flanking homologies. Consistently, integration of the transforming DNA next to the target in the genome was detected only in assays 2 and 3, in which targeted homology is disrupted with a large insertion and the transforming DNA fragment is either a little bit shorter or of same length as targeted region (assays 3 and 5). Again in agreement with this hypothesis, when *URA3* (1.16 kb) was used to delete a *Ty1* element from the *ura3-52* allele the fidelity of EOGT was only 60% and integration of the transforming DNA fragment next to the homology was observed in 10% of transformants [14]. In that assay the transforming DNA fragment integrated exclusively in the longer flanking homology in the terminator region of the *ura3* gene (0.82 kb; N-terminal homology was 0.34 kb). In the EOGT assays used here (Fig. 1A), with both flanking homologies of a similar size, integration of the transforming fragment was not biased suggesting that ends-out transforming fragment preferentially integrates in the region of a longer homology rather than in the terminator region.

4.2. BIR-induced targeted chromosome duplication during EOGT and EIGT is suppressed by Exo1 and Sgs1

TCD were detected in all EOGT assays described here (Fig. 1C) explaining the observation that approximately 8% of strains from the yeast knock-out library are aneuploidic for the targeted chromosome [78]. We have to stress that there was an observable decrease in the survival of the aneuploidic transformants during their passaging compared to gene targeting transformants. This is in agreement with physiological changes observed in aneuploidic yeast strains [79,80].

Although we have not directly demonstrated two copies of targeted chromosome in TCD transformants, we have shown that they contain two targeted regions (transformed and untransformed; Figs. 2B and 3B) which cannot be attributed to a duplication of a short chromosome region (Figs. S5B and C). Moreover, we have shown by Southern blotting of native chromosomes (Figs. 3C and S5B) that *URA3* and *ARG4* gene (for EOGT and EIGT, respectively) hybridize strictly to the targeted chromosome, and no additional molecules were detected. Finally, several TCD transformants (2 from the double *exo1Δ sgs1Δ* background in each ends-out and ends-in assay and 2–3 per each assay in wild type) were shown to have haploid DNA content confirming that TCD transformants are disomes for targeted chromosome. However, we cannot exclude that some of presumptive TCDs are diploids formed due to whole genome endoduplication prior or during transformation but not by cell fusion because it does not occur during lithium acetate transformation (Table S1) [81]. Additionally, we cannot

Table 3
The yield of each type of transformants in wild type, the *sgs1Δ* and *exo1Δ* single mutants and the *exo1Δ sgs1Δ* double mutant. First, the numbers of each type of transformation events obtained in wild type in assay 5 were normalized to the total of 100 transformants (Fig. 3D). Second, the total number of transformants obtained from each mutant was normalized according to the increased transformation efficiency in each mutant (Fig. 3A, assay 5), and finally, yield of each type of transformants in each mutant was calculated using data presented in Fig. 3D.

Transformation event	Assay 5							
		Wild type		*exo1Δ*		*sgs1Δ*		*exo1Δ sgs1Δ*
Successful gene targeting		94		116		1108		43
Aberrant events	Integration next to the targeted region (Int)		2		2		30	0
	Targeted chromosome duplications (TCD)	6	3	4	1	42	6	3057 2893
	Illegitimate integrations (Ille)		1		1		6	164
	Total	100		120		1150		3100

exclude that a small percentage of TCD transformants were due to spontaneous duplication of a targeted chromosome, followed by successful gene targeting but the absence of such events in the *pol32Δ* mutant (assay 5; Fig. 1D) clearly demonstrates that most, if not all, observed chromosome duplications occur by BIR [47]. It is also possible that some TCDs contain even three copies of targeted chromosome due to transformation fragment mediated chromosome missegregation [19] followed by BIR.

The fidelity of EOGT was significantly lower in *pol32Δ* mutant than in wild type due to striking increase of illegitimate integration of the transforming DNA. This effect could be consequence of interaction of transforming DNA with single stranded gaps accumulated in *pol32Δ* [56]. Moreover, it could be enhanced if gene targeting in assay 5 occurs by assimilation of ss DNA (see above) because illegitimate integration of single stranded transforming DNA can be further encouraged due to pairing with microhomology in single stranded gaps.

Due to reduced extensive DNA resection in the *exo1Δ sgs1Δ* double mutant [31–33] the transforming DNA fragment is more stable resulting in the synergistic increase of the transformation efficiency during both EIGT [41] and EOGT [42]. In assays described here (Fig. 3A) this effect is less pronounced and it depends on the type of intended genome modification, being higher for the EOGT assay 3 (replacement assay) than for the EOGT assay 5 (deletion assay). Inactivation of single *EXO1* or *SGS1* genes had only a minor influence on both the fidelity of gene targeting and the spectra of transformation events compared to the wild type (Fig. 3D). However, in the double mutant fidelity of EOGT decreased 65-fold compared to wild type (from 94.10% in the wild type to 1.38% in the double mutant).

To determine the influence of Exo1 and Sgs1 proteins on the yield of each type of transformants (Table 3) we normalized numbers of transformants obtained in assay 5 (Fig. 3D) according to the transformation efficiencies achieved in a given genetic backgrounds (Fig. 3A, assay 5). Data presented in Table 3 suggests that, although the frequency of gene targeting in the *exo1Δ sgs1Δ* double mutant, as determined by a molecular characterization of the obtained transformants, was only 1.38% percent, the yield of transformants dropped only to 50% compared to wild type strain (from 94 to 43, respectively). Interestingly, in the double *exo1Δ sgs1Δ* mutant there is a striking increase both in the yield of chromosome duplications (from 6/100 in wild type to 2893/3100) and in illegitimate integrations (from 1/100 in wild type to 164/3100, respectively). A similar increase in aberrant events in the *exo1Δ sgs1Δ* double mutant was also observed in the *met17::ADE2/MET17* assay (L.S. Symington, unpublished). Increased yield of integration of transforming DNA fragment next to the targeted region resulting in tandem repeats [14] in *sgs1Δ* mutant is in accordance with the results obtained by Mukherjee and Storici [82] showing that deletion of *SGS1* significantly increases frequency of gene amplification events initiated by small DNA fragments.

Due to lack of normal checkpoint response in the *exo1Δ sgs1Δ* double mutant we cannot exclude half-crossover on centromere-containing side and BIR toward the telomere while a truncated chromosome could initiate a secondary recombination event [83] or missegregation of sister chromatids due to the bridging activity of the transforming DNA fragment, as proposed by Svetec et al. [14] and Mukherjee and Storici [82] or formation of joint molecules due to inactivation of *SGS1* gene [84,85] followed by successful gene targeting on one chromatid/chromosome.

Chung et al. [42] showed that gene replacement increased from 72% in wild type cells to 99% in the *exo1Δ sgs1Δ* double mutant. Discrepancies between the results described by Chung et al. [42] and here could be explained either by specificity of EOGT assays or due to the fact that in their experimental system, targeted region (*THR4* gene) was located on the chromosome III between *MAT* and *HMR**a*** loci. Therefore, dense heterochromatin repressing *HMLα* and *HMR**a*** regions as well as chromatin dynamics that changes the accessibility of these two genes used as donors during *MAT* switching [86–89] could also affect gene targeting. In agreement with our results, it has already been shown that Exo1 and Sgs1 inhibit BIR in both chromosome-break repair assay [45] and chromosome fragmentation assay with DNA fragments either linearized *in vivo* or introduced in the cell by transformation [44]. The increase of yield of successful gene targeting in the absence of Sgs1 protein (Table 3) confirms that its 3′–5′ helicase activity can disrupt/abort recombination intermediate [43]. Moreover the increase of TCD in the *exo1Δ sgs1Δ* double mutant, but not in the respective single mutants, is in accordance with studies showing that Exo1 and Sgs1 proteins independently prevent BIR [44,45].

TCD has never been reported in EIGT assays. However, it was proposed that during DSB repair it is not necessary that both 3′-ends simultaneously invade in the homologous duplex. Furthermore, it was shown that double stranded gap on a replicative plasmid can be repaired using two target sequences, each one used as a template to extend one 3′-end [90]. Therefore, we presumed that EIGT might also initiate BIR and result in whole chromosome duplication. In the EIGT assay described here (Fig. 2A) the frequency of targeted chromosome duplication in wild type was 1.46%. Furthermore, in accordance to the results obtained in EOGT assays, the absence of Exo1 and Sgs1 proteins in EIGT assay strikingly decreased gene targeting fidelity to only 3.2% while the increase in the efficiency of transformation was due to increased proportion of TCD. These results clearly show that EIGT, as well as EOGT, can initiate duplication of a targeted chromosome and this aberrant transformation event is suppressed by Exo1 and Sgs1 proteins.

5. Conclusion

Precise genetic modification, using either EIGT or EOGT, can be associated with duplication of the targeted chromosome, which can easily go unnoticed if strains are not appropriately checked either by Southern blotting or by PCR. It is necessary to confirm both the presence of an expected, modified allele and the absence of a starting allele. Although it was proposed that the transient inactivation of homologues of *EXO1* and *SGS1* genes could be used to increase

transformation efficiency in higher eukaryotes [41,42], results presented here show that absence of Exo1 and Sgs1 proteins leads to BIR-induced chromosome duplication during both, ends-out and ends-in gene targeting.

Conflict of interest statement

The authors declare that there are no conflicts of interest.

Acknowledgements

This paper is dedicated to the memory of Zoran Zgaga (1956–2011). We would like to thank Krešimir Gjuračić, Petar T. Mitrikeski and Andrew W. Murray for stimulating discussion and Mark Prime for comments on the manuscript. This work was supported by grants from Croatian Ministry of Science, Education and Sports to Zoran Zgaga and I.-K. S. [grant number 058-0580477-225] and National Institutes of Health to L. S. S. [grant number R01 GM094386].

Appendix A. Supplementary data

Supplementary data associated with this article can be found, in the online version, at http://dx.doi.org/10.1016/j.dnarep.2014.07.004.

References

[1] R.J. Rothstein, One-step gene disruption in yeast, Methods Enzymol. 101 (1983) 202–211.
[2] T.L. Orr-Weaver, J.W. Szostak, R.J. Rothstein, Yeast transformation: a model system for the study of recombination, Proc. Natl. Acad. Sci. U. S. A. 78 (10) (1981) 6354–6358.
[3] T.L. Orr-Weaver, J.W. Szostak, R.J. Rothstein, Genetic applications of yeast transformation with linear and gapped plasmids, Methods Enzymol. 101 (1983) 228–245.
[4] J.R. Perera, A.V. Glasunov, V.M. Glaser, A.V. Boreiko, Repair of double-strand breaks in plasmid DNA in the yeast *Saccharomyces cerevisiae*, Mol. Gen. Genet. 213 (2–3) (1988) 421–424.
[5] V.M. Glaser, A.V. Glasunov, G.G. Tevzadze, J.R. Perera, S.V. Shestakov, Genetic control of plasmid DNA double-strand gap repair in yeast *Saccharomyces cerevisiae*, Curr. Genet. 18 (1) (1990) 1–5.
[6] A.V. Glasunov, V.M. Glaser, The influence of mutation rad57-1 on the fidelity of DNA double-strand gap repair in *Saccharomyces cerevisiae*, Curr. Genet. 34 (6) (1999) 430–437.
[7] M. Elias-Arnanz, A.A. Firmenich, P. Berg, *Saccharomyces cerevisiae* mutants defective in plasmid-chromosome recombination, Mol. Gen. Genet. 252 (5) (1996) 530–538.
[8] S. Bartsch, L.E. Kang, L.S. Symington, *RAD51* is required for the repair of plasmid double-stranded DNA gaps from either plasmid or chromosomal templates, Mol. Cell. Biol. 20 (4) (2000) 1194–1205.
[9] L.S. Symington, L.E. Kang, S. Moreau, Alteration of gene conversion tract length and associated crossing over during plasmid gap repair in nuclease-deficient strains of *Saccharomyces cerevisiae*, Nucleic Acids Res. 28 (23) (2000) 4649–4656.
[10] W. Leung, A. Malkova, J.E. Haber, Gene targeting by linear duplex DNA frequently occurs by assimilation of a single strand that is subject to preferential mismatch correction, Proc. Natl. Acad. Sci. U. S. A. 94 (13) (1997) 6851–6856.
[11] L.D. Langston, L.S. Symington, Gene targeting in yeast is initiated by two independent strand invasions, Proc. Natl. Acad. Sci. U. S. A. 101 (43) (2004) 15392–15397.
[12] L.D. Langston, L.S. Symington, Opposing roles for DNA structure-specific proteins Rad1, Msh2, Msh3, and Sgs1 in yeast gene targeting, EMBO J. 24 (12) (2005) 2214–2223.
[13] P.J. Hastings, C. McGill, B. Shafer, J.N. Strathern, Ends-in vs. ends-out recombination in yeast, Genetics 135 (4) (1993) 973–980.
[14] I.K. Svetec, A. Štafa, Z. Zgaga, Genetic side effects accompanying gene targeting in yeast: the influence of short heterologous termini, Yeast 24 (8) (2007) 637–652.
[15] S. Kunes, D. Botstein, M.S. Fox, Transformation of yeast with linearized plasmid DNA. Formation of inverted dimers and recombinant plasmid products, J. Mol. Biol. 184 (3) (1985) 375–387.
[16] S. Kunes, D. Botstein, M.S. Fox, Synapsis-mediated fusion of free DNA ends forms inverted dimer plasmids in yeast, Genetics 124 (1) (1990) 67–80.
[17] A. Malkova, E.L. Ivanov, J.E. Haber, Double-strand break repair in the absence of *RAD51* in yeast: a possible role for break-induced DNA replication, Proc. Natl. Acad. Sci. U. S. A. 93 (14) (1996) 7131–7136.
[18] D.M. Morrow, C. Connelly, P. Hieter, Break copy duplication: a model for chromosome fragment formation in *Saccharomyces cerevisiae*, Genetics 147 (2) (1997) 371–382.
[19] J.A. Kaye, et al., DNA breaks promote genomic instability by impeding proper chromosome segregation, Curr. Biol. 14 (23) (2004) 2096–2106.
[20] P. Manivasakam, S.C. Weber, J. McElver, R.H. Schiestl, Micro-homology mediated PCR targeting in *Saccharomyces cerevisiae*, Nucleic Acids Res. 23 (14) (1995) 2799–2800.
[21] A. Wach, A. Brachat, C. Alberti-Segui, C. Rebischung, P. Philippsen, Heterologous HIS3 marker and GFP reporter modules for PCR-targeting in *Saccharomyces cerevisiae*, Yeast 13 (11) (1997) 1065–1075.
[22] A.M. Bailis, S. Maines, Nucleotide excision repair gene function in short-sequence recombination, J. Bacteriol. 178 (7) (1996) 2136–2140.
[23] M. Gray, S.M. Honigberg, Effect of chromosomal locus, GC content and length of homology on PCR-mediated targeted gene replacement in *Saccharomyces*, Nucleic Acids Res. 29 (24) (2001) 5156–5162.
[24] M.G. Lee, L.H. Van der Ploeg, Homologous recombination and stable transfection in the parasitic protozoan *Trypanosoma brucei*, Science 250 (4987) (1990) 1583–1587.
[25] A.L. ten Asbroek, M. Ouellette, P. Borst, Targeted insertion of the neomycin phosphotransferase gene into the tubulin gene cluster of *Trypanosoma brucei*, Nature 348 (6297) (1990) 174–175.
[26] R.L. Barnes, R. McCulloch, *Trypanosoma brucei* homologous recombination is dependent on substrate length and homology, though displays a differential dependence on mismatch repair as substrate length decreases, Nucleic Acids Res. 35 (10) (2007) 3478–3493.
[27] D.G. Schaefer, J.P. Zryd, Efficient gene targeting in the moss *Physcomitrella patens*, Plant J. 11 (6) (1997) 1195–1206.
[28] Y. Kamisugi, A.C. Cuming, D.J. Cove, Parameters determining the efficiency of gene targeting in the moss *Physcomitrella patens*, Nucleic Acids Res. 33 (19) (2005) e173.
[29] Y. Kamisugi, et al., The mechanism of gene targeting in *Physcomitrella patens*: homologous recombination, concatenation and multiple integration, Nucleic Acids Res. 34 (21) (2006) 6205–6214.
[30] K.R. Folger, E.A. Wong, G. Wahl, M.R. Capecchi, Patterns of integration of DNA microinjected into cultured mammalian cells: evidence for homologous recombination between injected plasmid DNA molecules, Mol. Cell. Biol. 2 (11) (1982) 1372–1387.
[31] E.P. Mimitou, L.S. Symington, Sae2, Exo1 and Sgs1 collaborate in DNA double-strand break processing, Nature 455 (7214) (2008) 770–774.
[32] S. Gravel, J.R. Chapman, C. Magill, S.P. Jackson, DNA helicases Sgs1 and BLM promote DNA double-strand break resection, Genes Dev. 22 (20) (2008) 2767–2772.
[33] Z. Zhu, W.H. Chung, E.Y. Shim, S.E. Lee, G. Ira, Sgs1 helicase and two nucleases Dna2 and Exo1 resect DNA double-strand break ends, Cell 134 (6) (2008) 981–994.
[34] N.S. Amin, M.N. Nguyen, S. Oh, R.D. Kolodner, exo1-Dependent mutator mutations: model system for studying functional interactions in mismatch repair, Mol. Cell. Biol. 21 (15) (2001) 5142–5155.
[35] L. Maringele, D. Lydall, Telomerase- and recombination-independent immortalization of budding yeast, Genes Dev. 18 (21) (2004) 2663–2675.
[36] C. Cotta-Ramusino, et al., Exo1 processes stalled replication forks and counteracts fork reversal in checkpoint-defective cells, Mol. Cell 17 (1) (2005) 153–159.
[37] S. Gangloff, J.P. McDonald, C. Bendixen, L. Arthur, R. Rothstein, The yeast type I topoisomerase Top3 interacts with Sgs1, a DNA helicase homolog: a potential eukaryotic reverse gyrase, Mol. Cell. Biol. 14 (12) (1994) 8391–8398.
[38] G. Ira, A. Malkova, G. Liberi, M. Foiani, J.E. Haber, Srs2 and Sgs1-Top3 suppress crossovers during double-strand break repair in yeast, Cell 115 (4) (2003) 401–411.
[39] L. Wu, et al., The HRDC domain of BLM is required for the dissolution of double Holliday junctions, EMBO J. 24 (14) (2005) 2679–2687.
[40] Y. Yamana, et al., Regulation of homologous integration in yeast by the DNA repair proteins Ku70 and RecQ, Mol. Genet. Genomics 273 (2) (2005) 167–176.
[41] A. Štafa, I.-K. Svetec, Z. Zgaga, Inactivation of the *SGS1* and *EXO1* genes synergistically stimulates plasmid integration in yeast, Food Technol. Biotechnol. 43 (2005) 103–108.
[42] W.H. Chung, Z. Zhu, A. Papusha, A. Malkova, G. Ira, Defective resection at DNA double-strand breaks leads to de novo telomere formation and enhances gene targeting, PLoS Genet. 6 (5) (2010) e1000948.
[43] N. Sugawara, T. Goldfarb, B. Studamire, E. Alani, J.E. Haber, Heteroduplex rejection during single-strand annealing requires Sgs1 helicase and mismatch repair proteins Msh2 and Msh6 but not Pms1, Proc. Natl. Acad. Sci. U. S. A. 101 (25) (2004) 9315–9320.
[44] V.A. Marrero, L.S. Symington, Extensive DNA end processing by Exo1 and Sgs1 inhibits break-induced replication, PLoS Genet. 6 (7) (2010) e1001007.
[45] J.R. Lydeard, Z. Lipkin-Moore, S. Jain, V.V. Eapen, J.E. Haber, Sgs1 and Exo1 redundantly inhibit break-induced replication and de novo telomere addition at broken chromosome ends, PLoS Genet. 6 (5) (2010) e1000973.
[46] E. Johansson, S.A. MacNeill, The eukaryotic replicative DNA polymerases take shape, Trends Biochem. Sci. 35 (6) (2010) 339–347.
[47] J.R. Lydeard, S. Jain, M. Yamaguchi, J.E. Haber, Break-induced replication and telomerase-independent telomere maintenance require Pol32, Nature 448 (7155) (2007) 820–823.
[48] Z. Zgaga, Transformation of *Saccharomyces cerevisiae* with UV-irradiated single-stranded plasmid, Mutat. Res. 263 (4) (1991) 211–215.

[49] J. Sambrook, D.W. Russell, Molecular Cloning: A Laboratory Manual, Cold Spring Harbor Laboratory Press, Cold Spring Harbor, NY, 2001.
[50] C.B. Brachmann, et al., Designer deletion strains derived from *Saccharomyces cerevisiae* S288C: a useful set of strains and plasmids for PCR-mediated gene disruption and other applications, Yeast 14 (2) (1998) 115–132.
[51] F. Sherman, Getting started with yeast, Methods Enzymol. 350 (2002) 3–41.
[52] R.D. Gietz, R.H. Schiestl, High-efficiency yeast transformation using the LiAc/SS carrier DNA/PEG method, Nat. Protoc. 2 (1) (2007) 31–34.
[53] K. Gjuračić, Z. Zgaga, Illegitimate integration of single-stranded DNA in *Saccharomyces cerevisiae*, Mol. Gen. Genet. 253 (1–2) (1996) 173–181.
[54] A.C. Gerstein, H.J. Chun, A. Grant, S.P. Otto, Genomic convergence toward diploidy in *Saccharomyces cerevisiae*, PLoS Genet. 2 (9) (2006) e145.
[55] Y. Habraken, P. Sung, L. Prakash, S. Prakash, Binding of insertion/deletion DNA mismatches by the heterodimer of yeast mismatch repair proteins MSH2 and MSH3, Curr. Biol. 6 (9) (1996) 1185–1187.
[56] G.I. Karras, S. Jentsch, The *RAD6* DNA damage tolerance pathway operates uncoupled from the replication fork and is functional beyond S phase, Cell 141 (2) (2010) 255–267.
[57] F. Paques, J.E. Haber, Multiple pathways of recombination induced by double-strand breaks in *Saccharomyces cerevisiae*, Microbiol. Mol. Biol. Rev. 63 (2) (1999) 349–404.
[58] Y. Karpenshif, K.A. Bernstein, From yeast to mammals: recent advances in genetic control of homologous recombination, DNA Repair 11 (10) (2012) 781–788.
[59] L. Krejci, et al., Homologous recombination and its regulation, Nucleic Acids Res. 40 (13) (2012) 5795–5818.
[60] M. Aggarwal, R.M. Brosh Jr., Functional analyses of human DNA repair proteins important for aging and genomic stability using yeast genetics, DNA Repair (Amst.) 11 (4) (2012) 335–348.
[61] M. Klutstein, H. Shaked, A. Sherman, N. Avivi-Ragolsky, E. Shema, D. Zenvirth, A.A. Levy, G. Simchen, Functional conservation of the yeast and *Arabidopsis RAD54*-like genes, Genetics 178 (4) (2008) 2389–2397.
[62] H. Shaked, C. Melamed-Bessudo, A.A. Levy, High-frequency gene targeting in *Arabidopsis* plants expressing the yeast *RAD54* gene, Proc. Natl. Acad. Sci. U. S. A. 102 (34) (2005) 12265–12269.
[63] Y.I. Kwon, et al., Overexpression of OsRecQl4 and/or OsExo1 enhances DSB-induced homologous recombination in rice, Plant Cell Physiol. 53 (12) (2012) 2142–2152.
[64] D.G. Schaefer, et al., RAD51 loss of function abolishes gene targeting and de-represses illegitimate integration in the moss *Physcomitrella patens*, DNA Repair 9 (5) (2010) 526–533.
[65] E. Foureau, et al., Efficient gene targeting in a *Candida guilliermondii* non-homologous end-joining pathway-deficient strain, Biotechnol. Lett. 35 (7) (2013) 1035–1043.
[66] H. Bouabe, K. Okkenhaug, A protocol for construction of gene targeting vectors and generation of homologous recombinant embryonic stem cells, Methods Mol. Biol. 1064 (2013) 337–354.
[67] A. Kurosawa, et al., DNA Ligase IV and Artemis act cooperatively to suppress homologous recombination in human cells: implications for DNA double-strand break repair, PLOS ONE 8 (8) (2013) e72253.
[68] P. Hasty, J. Riveraperez, C. Chang, A. Bradley, Target frequency and integration pattern for insertion and replacement vectors in embryonic stem-cells, Mol. Cell. Biol. 11 (9) (1991) 4509–4517.
[69] W.J. Gong, K.G. Golic, Ends-out, or replacement, gene targeting in *Drosphila*, Proc. Natl. Acad. Sci. U. S. A. 100 (5) (2003) 2556–2561.
[70] S. Hacein-Bey-Abina, et al., *LMO2*-associated clonal T cell proliferation in two patients after gene therapy for SCID-X1, Science 302 (5644) (2003) 415–419.
[71] L. Fan, J. Moon, J. Crodian, P. Collodi, Homologous recombination in zebrafish ES cells, Transgenic Res. 15 (1) (2006) 21–30.
[72] K. D'Halluin, C. Vanderstraeten, E. Stals, M. Cornelissen, R. Ruiter, Homologous recombination: a basis for targeted genome optimization in crop species such as maize, Plant Biotechnol. J. 6 (1) (2008) 93–102.
[73] D.W. Russell, R.K. Hirata, Human gene targeting favors insertions over deletions, Hum. Gene Ther. 19 (9) (2008) 907–914.
[74] H.M. Kearney, D.T. Kirkpatrick, J.L. Gerton, T.D. Petes, Meiotic recombination involving heterozygous large insertions in *Saccharomyces cerevisiae*: formation and repair of large, unpaired DNA loops, Genetics 158 (4) (2001) 1457–1476.
[75] J.A. Clikeman, S.L. Wheeler, J.A. Nickoloff, Efficient incorporation of large (>2 kb) heterologies into heteroduplex DNA: Pms1/Msh2-dependent and -independent large loop mismatch repair in *Saccharomyces cerevisiae*, Genetics 157 (4) (2001) 1481–1491.
[76] L.E. Jensen, P.A. Jauert, D.T. Kirkpatrick, The large loop repair and mismatch repair pathways of *Saccharomyces cerevisiae* act on distinct substrates during meiosis, Genetics 170 (3) (2005) 1033–1043.
[77] P. Koren, I.K. Svetec, P.T. Mitrikeski, Z. Zgaga, Influence of homology size and polymorphism on plasmid integration in the yeast *CYC1* DNA region, Curr. Genet. 37 (5) (2000) 292–297.
[78] T.R. Hughes, et al., Widespread aneuploidy revealed by DNA microarray expression profiling, Nat. Genet. 25 (3) (2000) 333–337.
[79] E.M. Torres, et al., Effects of aneuploidy on cellular physiology and cell division in haploid yeast, Science 317 (5840) (2007) 916–924.
[80] J.M. Sheltzer, et al., Aneuploidy drives genomic instability in yeast, Science 333 (6045) (2011) 1026–1030.
[81] R.D. Gietz, R.H. Schiestl, A.R. Willems, R.A. Woods, Studies on the transformation of intact yeast cells by the LiAc/SS-DNA/PEG procedure, Yeast 11 (4) (1995) 355–360.
[82] K. Mukherjee, F. Storici, A mechanism of gene amplification driven by small DNA fragments, PLoS Genet. 8 (12) (2012) e1003119.
[83] A. Štafa, R.A. Donnianni, L.A. Timashev, A.F. Lam, L.S. Symington, Template switching during break-induced replication is promoted by the Mph1 helicase in *Saccharomyces cerevisiae*, Genetics 196 (4) (2014) 1017–1028.
[84] S.D. Oh, J.P. Lao, A.F. Taylor, G.R. Smith, N. Hunter, RecQ helicase, Sgs1, and XPF family endonuclease, Mus81-Mms4, resolve aberrant joint molecules during meiotic recombination, Mol. Cell 31 (3) (2008) 324–336.
[85] S.D. Oh, J.P. Lao, P.Y. Hwang, A.F. Taylor, G.R. Smith, N. Hunter, BLM ortholog, Sgs1, prevents aberrant crossing-over by suppressing formation of multichromatid joint molecules, Cell 130 (2) (2007) 259–272.
[86] P. Houston, P.J. Simon, J.R. Broach, The *Saccharomyces cerevisiae* recombination enhancer biases recombination during interchromosomal mating-type switching but not in interchromosomal homologous recombination, Genetics 166 (3) (2004) 1187–1197.
[87] E. Coic, et al., Dynamics of homology searching during gene conversion in *Saccharomyces cerevisiae* revealed by donor competition, Genetics 189 (4) (2011) 1225–1233.
[88] J.E. Haber, Mating-type genes and *MAT* switching in *Saccharomyces cerevisiae*, Genetics 191 (1) (2012) 33–64.
[89] J. Li, et al., Regulation of budding yeast mating-type switching donor preference by the FHA domain of Fkh1, PLoS Genet. 8 (4) (2012) e1002630.
[90] F. Paques, W.Y. Leung, J.E. Haber, Expansions and contractions in a tandem repeat induced by double-strand break repair, Mol. Cell. Biol. 18 (4) (1998) 2045–2054.